Wireless Personal Communications **4:** 299–314, 1997.

Combined Space Diversity Reception and Trellis Coding for Rayleigh Fading Channels

GUILLEM FEMENIAS[1] and RAMON AGUSTI[2]
[1]*Departament de Ciències Matemàtiques i Informàtica, Universitat de les Illes Balears (UIB), Palma de Mallorca, 07071 Spain;*
[2]*Departament de Teoria del Senyal i Comunicacions, Universitat Politècnica de Catalunya (UPC), Barcelona, 08080 Spain*
Tel.: 71173196; Fax: 71173003; E-mail: guillem@ipc4.uib.es

Abstract. Space diversity reception, in which several signals received at different antennas are combined, is a well known method that can be used to combat the effects of fading in wireless systems. Also, trellis coded modulation (TCM), when combined with interleaving of sufficient depth, is known to provide some form of time diversity that allows the achievement of good error performance in fading environments. In this paper we consider the analysis of the error performance of reference-based Maximal Ratio Combining (MRC) systems when used in conjunction with trellis-coded MPSK modulation techniques over a Rayleigh fading channel. We also consider the analysis of MRC trellis-coded MPSK systems with conventional differential detection. The results are obtained by using a combination of theoretical analysis and simulation. Exact and near-exact expressions for the pairwise error-event probability in Rayleigh fading are derived. Monte-Carlo simulation results, which are more indicative of the exact system performance, are also given.

Key words: Trellis coding, space diversity, Rayleigh fading, pilot tone aided detection.

1. Introduction

Mobile radio communication systems have received considerable attention in recent years. The mobile radio channel is a multipath propagation medium, and hence if a relatively low bit rate signal with a bandwidth much smaller than the coherence bandwidth of the multipath channel is transmitted, signal envelope variation (multiplicative fading) and random FM noise will produce high error rates even with high average signal to noise ratios and place a lower limit on the achievable bit error rate (BER). As it is well known, the use of space diversity systems provides significant improvement in communications when transmitting through a fading propagation medium. If the antenna spacing is chosen so that the individual signals are uncorrelated then, each of the K antennas in the diversity array will provide an independent signal to the K-branch diversity combiner. A variety of techniques are available to perform the combining process and to capitalize on the uncorrelated fading exhibited by the K antennas in the space-diversity array [1, 2]. In maximal ratio combining (MRC) the K signals, after being cophased, are weighted proportionally to their signal voltage to noise power ratios and then summed. Of all diversity linear-combining schemes, maximal ratio combining is considered optimum in that it provides the highest average output signal to noise ratio and the lowest probability of deep fades [2]. To assist with the demodulation of MPSK signals and perform MRC in a fading environment, it is common practice to incorporate a reference signal (pilot symbols [3] or pilot tones [4]) alongside the transmitted data symbols. This allows the random FM noise and envelope fluctuations caused by multipath fading to be accurately tracked and eliminated, thus overcoming the irreducible error floor associated with data transmission over fading channels.

Trellis coded modulation (TCM), although originally developed for telephone channels [5], has received also considerable interest in the field of mobile radio [6–14]. The primary advantage of TCM over modulation schemes employing traditional error correction coding is its ability to achieve increased power efficiency without the customary expansion of bandwidth introduced by the coding process. Furthermore, when combined with interleaving of sufficient depth, TCM is known to provide some form of time diversity that allows the error rate to decrease with SNR faster than the inverse law commonly found on Rayleigh fading channels. Thus any fading channel that is both power-limited and bandwidth-limited would be ideally suited to TCM.

There are different methods that can be used to evaluate the performance of Trellis Coded Modulation schemes over Rayleigh fading channels. Chernoff upper bound combined with the *pair state generalized transfer function bound* approach [11] or the *modified state transition diagram transfer function bound* approach [15] has been widely used. However, this upper bound, although readily determined, is too loose over normal SNR ranges of interest. In their paper, J.K. Cavers and P. Ho [9] provide an exact expression for the pairwise error-event probability of TCM operating on a Rayleigh-fading channel. For short error events, this expression is easily computed and thus the procedure is effective. However, its complexity grows rapidly with the length of the error event path and with the order of diversity [12]. In [10] R.G. McKay et al. present an asymptotically tight upper bound based upon a simple modification to the standard transfer function/union-Chernoff bound that is combined with the exact solution for the pairwise error-event probability. This technique consists of deriving a tight upper bound using the exact pairwise error-event probabilities for m of the most dominant error events, in terms of asymptotic contribution to P_b, from the code trellis, and a weaker union-Chernoff bound for all remaining error-events. Obviously, the greater the number of error events considered in the set of "most dominant error-events" the tighter the upper bound will be, but at the expense of increasing the complexity.

In this paper we shall consider the performance analysis of a reference-based MRC system when used in conjunction with trellis-coded MPSK modulation techniques over a Rayleigh fading channel. This combined scheme, incorporating a reference signal, has not been so far considered. As a baseline performance measure we shall also include the analysis of MRC trellis-coded MPSK systems with conventional differential detection. The results shall be obtained by using a combination of theoretical analysis and simulation. In particular, the rate 2/3, four-state Du/Vucetic/Zhang code [13], implemented by means of a systematic encoder with feedback, will be analyzed. In performing the analysis a number of simplifying assumptions will be made. First, a theoretically ideal block interleaving/deinterleaving of channel signal will be assumed in order that the channel may be considered as memoryless. This assumption leads to independent fading of the adjacent demodulated symbols and allows for considerable simplification of the analysis. Second, it will also be assumed that fading over one baud interval may be represented by a single fading amplitude. Finally, although all simulation results will reflect a finite decoding delay of six times the convolutional encoder constraint length, an infinite decoding delay will be assumed in the analysis of the Viterbi decoding process.

The paper is organized as follows. The system and analysis models used in this study are described in Section 2. The average bit error probability bounds for both pilot tone aided predetection diversity coherent systems and postdetection diversity differential detection systems is then derived in Section 3. Also shown in Section 3 are some of our simulation results. Finally, discussion and the conclusions of this study are given in Section 4.

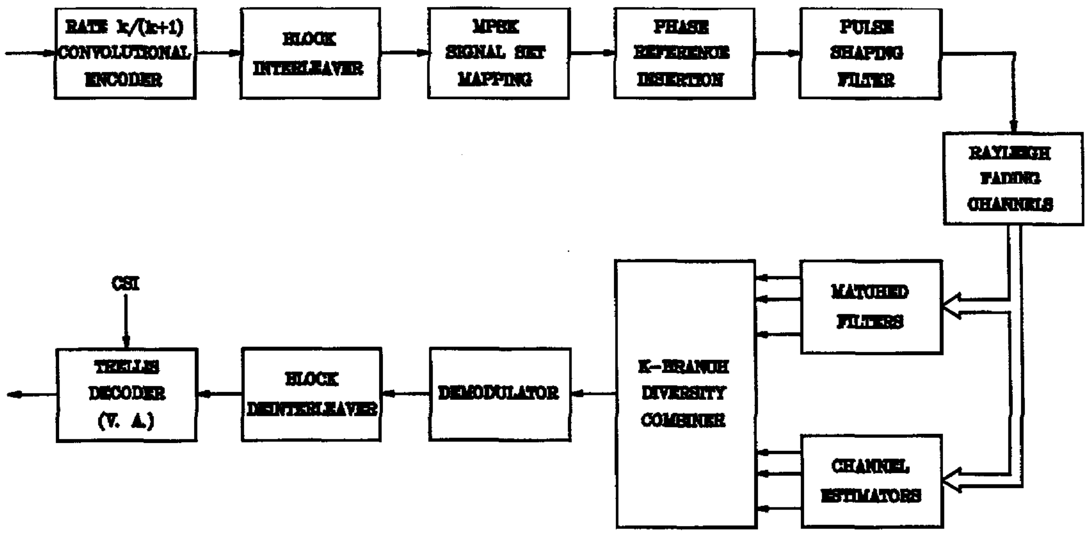

Figure 1. Baseband system model of the trellis coded system.

2. System and Analysis Models

The baseband system model under investigation is illustrated by the block diagram in Figure 1. Input bits (representing data or digitally encoded speech) at rate R_b are encoded by a rate $k/(k+1)$ trellis encoder producing an encoded symbol stream at rate $[(k+1)/k]R_b$. Trellis coded symbols (groups of $k+1$ bits) are next mapped, according to the *mapping by set partitioning rules* [5], onto an MPSK ($M = 2^{k+1}$) channel signal set and block interleaved to *randomize* the distribution of symbols affected by amplitude fading of duration greater than one symbol period. Following the interleaving process a phase reference signal is added to the data bearing signal. The composite signal is then pulse shaped and transmitted. Transmitted signal is faded and corrupted by AWGN passing through the fading channel. The received signal in each diversity branch is simultaneously passed to a matched filter and to a channel estimator. In-phase and quadrature components are combined, demodulated, quantized for soft decision and block deinterleaved. Using these quantized symbols, the Viterbi decoder detects the transmitted sequence based on maximum likelihood estimation.

For a received sequence of length N, $Y_N = (y_1, \dots, y_N)$, the metric between Y_N and any transmitted signal sequence $X_N = (x_1, \dots, x_N)$, is of the form $m(Y_N, X_N; Z_N)$ if side information is available and $m(Y_N, X_N)$ if it is not. The metric is used by the decoder to make decisions as to which sequence was transmitted given the corresponding channel output sequences. Whatever metric is selected, to simplify the decoder processing complexity, it is required to have an additive property, i.e.,

$$m(Y_N, X_N; Z_N) = \sum_{n=1}^{N} m(y_n, x_n; z_n). \tag{1}$$

Letting $m(Y_N, X_N; Z_N)$ denote the coding decision metric, the decoder incorrectly decides that the transmitted coded sequence is $\hat{X}_N \neq X_N$ when

$$m(Y_N, X_N; Z_N) \leq m(Y_N, \hat{X}_N; Z_N), \tag{2}$$

with a probability $P(X_N \rightarrow \hat{X}_N)$ which is called the *pairwise error probability*. By our previous assumptions

$$P(X_N \rightarrow \hat{X}_N) = \Pr(m(Y_N, \hat{X}_N; Z_N) \geq m(Y_N, X_N; Z_N) \mid X_N) = \Pr(f \geq 0 \mid X_N), \quad (3)$$

where

$$f = m(Y_N, \hat{X}_N; Z_N) - m(Y_N, X_N; Z_N). \quad (4)$$

An upper bound on the average bit error probability is obtained from $P(X_N \rightarrow \hat{X}_N)$ as [16]

$$P_b \leq \sum_{N=L_s}^{\infty} \sum_{X_N} \sum_{\hat{X}_N} a(X_N, \hat{X}_N) p(X_N) P(X_N \rightarrow \hat{X}_N), \quad (5)$$

where $a(X_N, \hat{X}_N)$ is the number of bit errors occurring when X_N is transmitted and $\hat{X}_N$ is chosen by the decoder, $p(X_N)$ is the a priori probability of transmitting X_N and L_s is the Hamming distance of the shortest error event.

3. Average Bit Error Probability Bounds

3.1. Pilot Tone Aided Predetection Diversity Coherent Systems

In order to have an accurate channel estimator at the receiver, a pilot signal can be sent along with the data bearing signal. The pilot signal can be a tone (or multiple tones) or it can be a sequence of symbols that are inserted periodically into the data bearing signal. Anyway, as was shown in [14], both systems provide the same performance for a given system power and information throughput. With a reference pilot tone signal, the baseband equivalent of the transmitted signal is

$$x(t) = B + \sum_n x_n q(t - nT), \quad (6)$$

where B represents the reference signal, $x_n = Ae^{j\phi_n}$, T is the symbol period and $q(t)$ represents the complex impulse response of a pulse shaping filter that satisfies Nyquist's criterion for zero intersymbol interference and has unity energy. It is assumed that the power spectrum of the data bearing signal has a spectral null that allows for the insertion and the extraction of the pilot.

Assuming, in general, a K branch diversity system, the baseband equivalent of the received signal on the kth receiver ($k = 1, 2, \ldots, K$) can be expressed as

$$r_k(t) = \chi_k(t) x(t) + \nu_k(t), \quad (7)$$

where $\nu_k(t)$, which represents the additive thermal noise at the receiver front-end, is a zero-mean complex Gaussian noise process with single-sided power spectral density N_0 and

$$\chi_k(t) = \rho_k(t) \exp[j\Psi_k(t)] \quad (8)$$

which represents the multiplicative Rayleigh fading characteristic of the channel, is a normalized (unit mean-square value), stationary, zero-mean complex Gaussian process. As shown in Figure 1, the received signal is simultaneously passed to a matched filter with an impulse response equal to $q^*(-t)$ and to a channel estimator that, in this case, is simply a pilot extraction filter with a frequency response

$$H(f) = \begin{cases} 1 & -B_p/2 \leq f \leq B_p/2 \\ 0 & \text{otherwise} \end{cases}. \tag{9}$$

Note that the bandwidth of the filter must be wide enough to allow the fading to pass through undistorted, that is, it must be at least twice the maximum Doppler shift, f_d. In the following analysis it will be assumed that a filter with bandwidth $B_p \geq 2f_d$ is used. Thus, the data bearing signal and the pilot signal at the output of the matched filter and pilot extraction filter can be expressed as

$$w_k(t) = \chi_k(t) \sum_n x_k h(t - nT) + n_k(t) \tag{10}$$

and

$$p_k(t) = \chi_k(t) B + v_k(t), \tag{11}$$

respectively, where $h(t) = q(t) * q^*(-t)$ represents the overall impulse response of the system for a perfect non selective transmission medium and $n_k(t)$ and $v_k(t)$ are zero mean complex Gaussian noise processes. Note that $n_k(t)$ is independent of $v_k(t)$ due to the fact that they are output noise processes of two filters whose frequency responses do not overlap. Using the pilot tone signals to cophase and weight the data bearing signals, the combined signal can be written as

$$g(t) = \sum_{k=1}^{K} w_k(t) p_k^*(t). \tag{12}$$

The signal at the output of the maximal ratio combiner is sampled by an A/D converter at time $t_n = nT + \tau$, where $-T/2 \leq \tau \leq T/2$ determines the sampling instant. Assuming a perfect clock recovery, $\tau = 0$, the complex sample at the output of the deinterleaver will be given by

$$y_n = \sum_{k=1}^{K} w_{k,n} p_{k,n}^*, \tag{13}$$

where, for simplicity of notation, we have dropped the delay introduced by the interleaving/deinterleaving process.

A soft Viterbi decoder performing maximum-likelihood sequence estimation (MLSE) will select the codeword for which the a posteriori probability is the largest. With the assumption of equally probable codeword and ideal interleaving, this is equivalent to choosing the codeword whose branch metrics are

$$m(y_n, x_n; z_n) = -\left| \sum_{k=1}^{K} w_{k,n} p_{k,n}^* - x_n \right|^2. \tag{14}$$

Substituting (14) into (4), the decision variable f can be expressed as a special case of the quadratic form given by Cavers et al. [9, eqs. (10) and (11)] as follows:

$$f = \sum_{n=1}^{N} \sum_{k=1}^{K} [A_n |p_{k,n}|^2 + B_n |w_{k,n}|^2 + C_n p_{k,n} w_{k,n}^* + C_n^* p_{k,n}^* w_{k,n}] \tag{15}$$

with $A_n = B_n = 0$ and $C_n = (\hat{x}_n - x_n)$. In a Rayleigh fading channel, $p_{k,n}$ and $w_{k,n}$ are zero-mean Gaussian distributed random variables when conditioned on the codeword. Furthermore, assuming a perfect interleaving/deinterleaving process and an antenna spacing such that the individual signals are uncorrelated, f in (15) will be a double sum of independent quadratic forms of zero-mean complex Gaussian random variables. The pdf of f is not an elementary function but its characteristic function is given by [17, Appendix 4B] as

$$G_f(jt) = \prod_{n\in\eta}\prod_{k=1}^{K} \frac{-t_{1n}t_{2n}}{(t-jt_{1n})(t-jt_{2n})}, \tag{16}$$

where $\eta = \{n : x_n \neq \hat{x}_n\}$,

$$t_{1n} = \omega_n - \sqrt{\omega_n^2 - t_{1n}t_{2n}}, \qquad t_{2n} = \omega_n + \sqrt{\omega_n^2 - t_{1n}t_{2n}} \tag{17}$$

with

$$\begin{aligned} t_{1n}t_{2n} &= \frac{-1}{(\mu_{pp}\mu_{ww} - |\mu_{pw}|^2)|C_n|^2}, \\ \omega_n &= \frac{C_n\mu_{pw}^* + C_n^*\mu_{pw}}{2(\mu_{pp}\mu_{ww} - |\mu_{pw}|^2)|C_n|^2} \end{aligned} \tag{18}$$

and

$$\begin{aligned} \mu_{pp} &= E\{|p_{k,n}|^2\} = B^2 + 2B_pN_0, \\ \mu_{ww} &= E\{|w_{k,n}|^2\} = A^2 + 2N_0, \\ \mu_{pw} &= E\{p_{k,n}^* w_{k,n}\} = ABe^{j\phi_n}, \\ |C_n|^2 &= A^2|e^{j\hat{\phi}_n} - e^{j\phi_n}|^2 = A^2 d_n^2. \end{aligned} \tag{19}$$

By substituting all the variables in (19) into (18), we have

$$\begin{aligned} t_{1n}t_{2n} &= \frac{-(1+r)}{8E_sB_pN_0^2d_n^2\left[\frac{E_s}{N_0}\left(\frac{r+B_pT}{B_pT(1+r)}\right)+1\right]}, \\ \omega_n &= 8B_pN_0^2\left(\frac{T(1+r)}{2rE_s}\right)^{1/2}\left[\frac{E_s}{N_0}\left(\frac{r+B_PT}{B_pT(1+r)}\right)+1\right], \end{aligned} \tag{20}$$

where $E_s = (A^2 + B^2T)/2$ is the equivalent energy per MPSK symbol and $r = B^2T/A^2$ is the pilot to signal power ratio.

The pairwise error probability can be expressed in terms of $G_f(jt)$ as [17, Appendix 4B]

$$P(X_N \to \hat{X}_N) = \Pr(f \geq 0 \mid X_N) = \frac{-1}{2\pi j}\int_{-\infty+j\varepsilon}^{\infty+j\varepsilon} \frac{G_f(jt)}{t}\,\mathrm{d}t, \tag{21}$$

where ε is a small positive number. Substituting (16) in (21) and closing the path of integration with a semicircle of radius $R \to \infty$ we have that, except for a finite number of poles, the function $G_f(jt)/t$ is regular in the region bounded by the closed path. Thus, based on the theorem of residues from the theory of functions of a complex variable, the integral in (21)

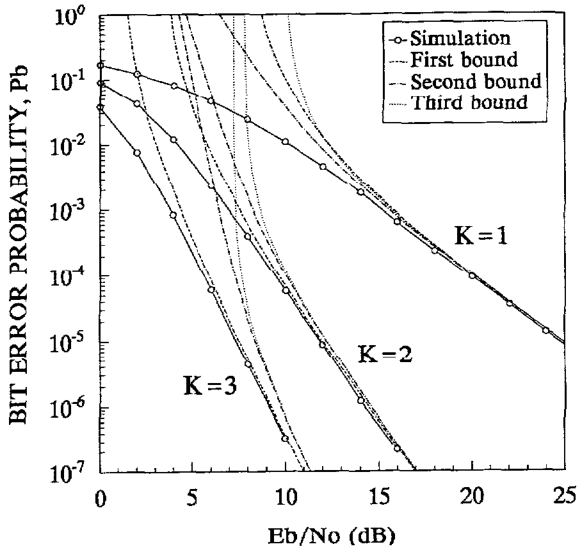

Figure 2. Bit error probability of a K-branch predetection MRC Du/Vucetic/Zhang four state TCM–8PSK system in a Rayleigh fading channel with pilot tone aided detection and a normalized fading rate of 0.01.

will be equal to the summation of all residues at the poles on the right-hand plane (RHP) of the following equation:

$$P(X_N \to \hat{X}_N) = -\sum \text{Residue}\{G_f(s)/s\}_{\text{RHP}_{\text{poles}}}, \tag{22}$$

where $G_f(s)$ is the two-sided Laplace transform of the pdf of f which can be written as

$$G_f(s) = \prod_{n \in \eta} \prod_{k=1}^{K} \frac{t_{1n} t_{2n}}{(s - t_{1n})(s - t_{2n})}, \tag{23}$$

where t_{1n} and t_{2n} are the left-hand plane (LHP) and the right-hand plane (RHP) poles, respectively. This method, although exact and mathematically simple, does not lend itself to the evaluation of an upper union bound on the bit error probability via the classical transfer function bound approach and, in fact, this is not considered a practical approach for evaluating functions with a large number of poles of high order; so, rather than accounting for error event paths of all lengths, approximations or upper bounding procedures that consider only a small set of short error events have been studied [9, 10, 12]. Two different bandwidth of the pilot filter, $B_pT = 0.02$ and 0.06, corresponding to a maximum normalized fading rate $f_dT = 0.01$ and 0.03, respectively, are considered in Figures 2 and 3, where simulation and analysis results of the 4-state Du/Vucetic/Zhang code TCM system are presented. In deriving this upper bound (First bound), the approach outlined in [12] has been applied considering error-events having diversity two and three in the set of "most dominant error-events" and using the Chernoff bound calculated in the Appendix to derive the pairwise error-event probability for all remaining error-events. For each value of B_pT, an optimum value for the energy ratio r has been derived. It can be observed that the analytical upper bound and simulation results are very close in all cases when the average bit error probability is less than 10^{-3}.

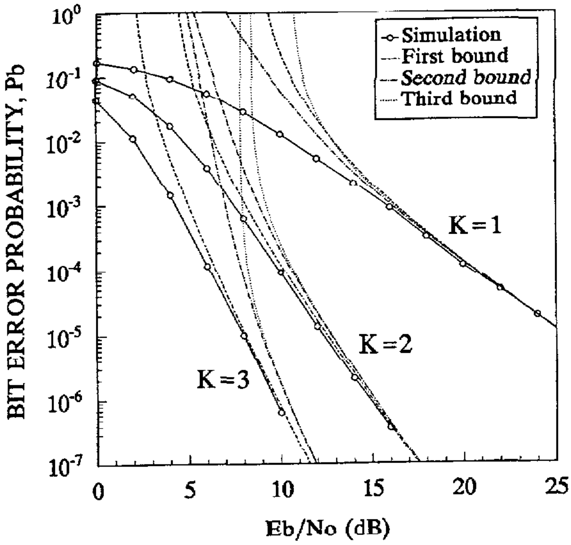

Figure 3. Bit error probability of a K-branch predetection MRC Du/Vucetic/Zhang four state TCM–8PSK system in a Rayleigh fading channel with pilot tone aided detection and a normalized fading rate of 0.03.

For both high signal and pilot to noise ratios, then $t_{1n}t_{2n} \ll \omega_n$ and thus (22) can be approximated by

$$P(X_N \to \hat{X}_N) \simeq \left(\prod_{n\in\eta}\prod_{k=1}^{K} t_{1n}t_{2n}\right) \sum \text{Residue}\left[-s^{-L_\eta K-1}(s-2\omega_n)^{-L_\eta K}\right]_{\text{RHP}_{\text{poles}}}, \quad (24)$$

where L_η is equal to the number of elements in the set η. Therefore, the following expression for the average bit error probability upper bound can be obtained

$$P_b \leq \sum_{N=L_s}^{\infty} \sum_{X_N} \sum_{\hat{X}_N} a(X_N, \hat{X}_N) p(X_N) C_{L_\eta K} \prod_{n\in\eta} \left[\frac{B_pT\left[\frac{E_s}{N_0}\left(\frac{r+B_pT}{B_pT(1+r)}\right)+1\right]}{\frac{r}{(1+r)^2}\left(\frac{E_s}{N_0}\right)^2 d_n^2}\right]^K, \quad (25)$$

where

$$C_{L_\eta K} = \frac{(2L_\eta K-1)!}{(L_\eta K)!(L_\eta K-1)!}\,. \quad (26)$$

Optimizing (25) over r we get

$$r_{\text{opt}} = \left(\frac{\frac{E_s}{N_0}+1}{\frac{E_s}{N_0}(B_pT)^{-1}+1}\right)^{1/2}. \quad (27)$$

Figures 2 and 3 also show the analysis results of this upper bound (Second bound). The summations have been performed over all error events of length up to 8.

A looser upper bound (Third bound) can be obtained by observing that [14]

$$\frac{1}{\alpha}\,2^{2L_\eta K} \geq C_{L_\eta K}, \quad (28)$$

where

$$\alpha = 2^{2L_sK} \frac{(L_sK)!(L_sK-1)!}{(2L_sK-1)!} . \tag{29}$$

By substituting α in (25), this gives another bound for the bit error probability

$$P_b \geq \sum_{N=L_s}^{\infty} \sum_{X_N} \sum_{\hat{X}_N} \frac{a(X_N, \hat{X}_N)p(X_N)}{\alpha} \prod_{n\in\eta} \left[\frac{4B_pT \left[\frac{E_s}{N_0} \left(\frac{r+B_pT}{B_pT(1+r)} \right) + 1 \right]}{\frac{r}{(1+r)^2} \left(\frac{E_s}{N_0} \right)^2 d_n^2} \right]^K . \tag{30}$$

This expression enables the use of the classical transfer function bound approach to evaluate the union upper bound on the average bit error probability. From (30) it can be seen that at high SNR the probability error is inversely proportional to the L_sKth power of the SNR. This is the combined effect of space diversity and intrinsic time diversity of TCM. Figures 2 and 3 show this upper bound using the transfer function approach. It can be observed that this upper bound is asymptotically very tight.

3.2. Ideal Predetection Diversity Coherent Systems

In the ideal coherent systems it is assumed that no pilot signal is transmitted along with the data bearing signal and that the channel estimator at the receiver is able to obtain an exact estimate of the channel from the data bearing signal itself. In this case the baseband equivalent of the transmitted signal and the output of the channel estimator can be written as

$$x(t) = \sum_n x_n q(t-nT) \tag{31}$$

and

$$p_k(t) = \chi_k(t), \tag{32}$$

respectively. Thus,

$$t_{1n}t_{2n} = \frac{-1}{4E_sN_0d_n^2}, \qquad \omega_n = \frac{-1}{4N_0}, \tag{33}$$

where $E_s = A^2/2$ is the equivalent energy per MPSK symbol. Using these expressions, the approach outlined in [12] has been applied to obtain the results presented in Figure 4. These results have also been obtained by considering error events having diversity two and three in the set of "most dominant error events" and using the Chernoff bound calculated in [12, Appendix A] to derive the pairwise error-event probability for all remaining error-events. Notice that, with an appropriate choice of the bandwidth of the pilot filter extractor, the performance of the pilot tone aided coded scheme is quite close to that of the idealized system for normalized fading rates less than 0.03.

For high signal to noise ratios, the following expression for the average bit error probability upper bound can be obtained

$$P_b \leq \sum_{N=L_s}^{\infty} \sum_{X_N} \sum_{\hat{X}_N} a(X_N, \hat{X}_N)p(X_N)C_{L_\eta K} \prod_{n\in\eta} \left[\frac{E_s}{N_0} d_n^2 \right]^{-K} . \tag{34}$$

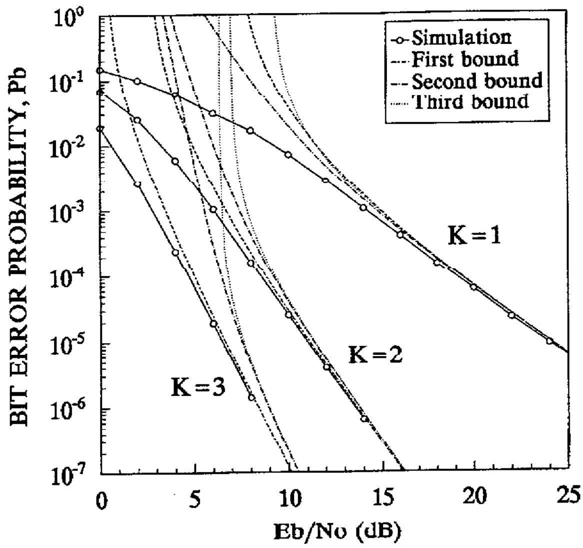

Figure 4. Bit error probability of a K-branch predetection MRC Du/Vucetic/Zhang four state TCM–8PSK system in a Rayleigh fading channel with perfect CSI.

By substituting (29) in (34), this gives a third upper bound for the bit error probability

$$P_b \leq \sum_{N=L_s}^{\infty} \sum_{X_N} \sum_{\hat{X}_N} \frac{a(X_N, \hat{X}_N)p(X_N)}{\alpha} \prod_{n\in\eta} \left[\frac{E_s}{4N_0} d_n^2\right]^{-K}. \tag{35}$$

Figure 4 also shows the analytical results obtained through the application of these upper bounds.

3.3. Postdetection Diversity Differential Detection Systems

In this case, the nth element of the interleaved trellis coded symbol sequence X_N, namely x_n, is the phasor representation of the MPSK coded symbol $\Delta\phi_n$ assigned by the mapper in the nth transmission interval. It can be written as

$$x_n = e^{j\Delta\phi_n}. \tag{36}$$

Before transmission over the channel, the mapper output symbol sequence, X_N, is differentially encoded producing the sequence μ_N. In phasor notation, the MDPSK coded symbol in the nth transmission interval can be written as

$$\mu_n = \mu_{n-1}x_n = Ae^{j(\phi_{n-1}+\Delta\phi_n)} = Ae^{j\phi_n} \tag{37}$$

and the baseband equivalent of the transmitted signal is

$$\mu(t) = \sum_n \mu_n q(t - nT). \tag{38}$$

Assuming a K branch diversity system and the use of an ideal automatic frequency control (AFC), that is, a perfect compensation of frequency offsets between emitter and receiver local oscillators, the complex envelope of the received signal and the signal at the output of the reception filter in the kth receiver ($k = 1, 2, \ldots, K$) can be expressed as

$$r_k(t) = \chi_k(t)\mu(t) + \nu_k(t) \tag{39}$$

and

$$w_k(t) = \chi_k(t)\sum_n \mu_n h(t - nT) + n_k(t) = \chi_k(t)\mu_f(t) + n_k(t), \tag{40}$$

respectively. In a postdetection diversity receiver, including the differential detection function [18], each branch input signal is multiplied by its delayed replica, with the time delay $t_d = T$ for differential detection. The combiner output is sent to the demodulator to obtain in-phase and quadrature channel outputs. After filtering, these signals are sampled by an A/D converter. Assuming a perfect clock recovery, the complex sample at the deinterleaver output, that is, the nth element of the output sequence Y_N corresponding to the input sequence X_N will be given by

$$y_n = \sum_{k=1}^{K} w_{k,n-1}^* w_{k,n}. \tag{41}$$

Using these quantized symbols, the trellis decoder, implemented as a Viterbi algorithm with a metric depending upon whether or not channel state information (CSI) is provided, detects the transmitted sequence based on maximum likelihood estimation. The optimum (maximum-likelihood) metric depends on the joint two-dimensional (amplitude and phase) statistics of a received sequence and is quite complicated to implement [7]. Assuming a soft Viterbi decoding based on the much simpler Gaussian metric, i.e.,

$$m(y_n, x_n; z_n) = -\left|\sum_{k=1}^{K} w_{k,n} w_{k,n-1}^* - A^2 x_n\right|^2 \tag{42}$$

the differential detection system can be analyzed as the coherent one and using the previous received symbol as a reference. That is, expressions (16–18) and (21–23) can be used with

$$\begin{aligned}
\mu_{pp} &= E\{|w_{k,n-1}|^2\} = A^2 + 2N_0, \\
\mu_{ww} &= E\{|w_{k,n}|^2\} = A^2 + 2N_0, \\
\mu_{pw} &= E\{w_{k,n-1}^* w_{k,n}\} = A^2 x_n J_0(2\pi f_d T), \\
|C_n|^2 &= A^4|\hat{x}_n - x_n|^2 = A^4 d_n^2,
\end{aligned} \tag{43}$$

where f_d is the maximum Doppler frequency and $J_0(\cdot)$ is the Bessel function of order zero. By substituting all the variables in (43) into (18), we have

$$\begin{aligned}
t_{1n}t_{2n} &= \frac{-1}{16E_s^2 N_0^2 d_n^2 \left[\left(\frac{E_s}{N_0}\right)^2 [1 - J_0^2(2\pi f_d T)] + 2\left(\frac{E_s}{N_0}\right) + 1\right]}, \\
\omega_n &= \frac{-J_0(2\pi f_d T)}{8N_0^2 \left[\left(\frac{E_s}{N_0}\right)^2 [1 - J_0^2(2\pi f_d T)] + 2\left(\frac{E_s}{N_0}\right) + 1\right]},
\end{aligned} \tag{44}$$

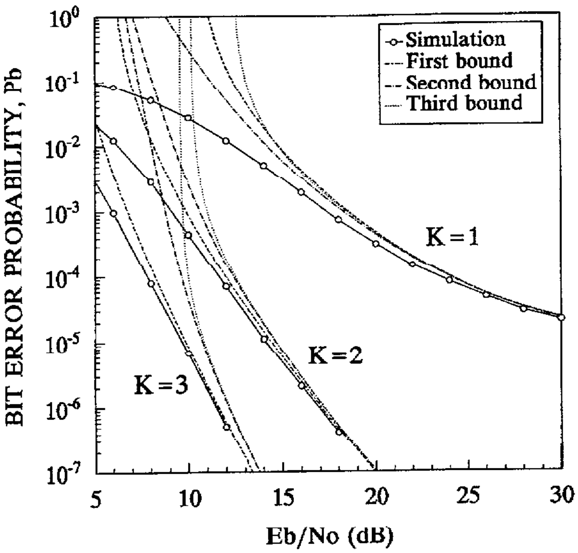

Figure 5. Bit error probability of a K-branch postdetection MRC Du/Vucetic/Zhang four state TCM–8PSK system in a Rayleigh fading channel with differential detection and a normalized fading rate of 0.01.

where $E_s = A^2/2$ is the equivalent energy per MDPSK symbol. Using these expressions to derive the pairwise error-event probability of the "most dominant error events" and the Chernoff bound calculated in Appendix to derive the pairwise error-event probability for all remaining error-events, the approach outlined in [12] has been applied to obtain the results presented in Figures 5 and 6. Normalized fading rates of 0.01 and 0.03 have been considered. It can be seen that the system performance deteriorates as the normalized fading rate increases and an average bit error floor is clearly shown for fast Rayleigh fading. Comparing the irreducible error probability obtained without diversity with that obtained with two or three antenna diversity, we conclude the space diversity applies to the irreducible error floor as well. The upper bound is very tight for slow fading and high space diversity orders and becomes less accurate as the fading rate increases.

For both $E_s/N_0 \gg 0$ and $J_0(2\pi f_d T) \simeq 1$, then $t_{1n}t_{2n} \ll \omega_n$ and thus expression (22) can be approximated by expression (24). Therefore, the following expression for the second upper bound on the average bit error probability is obtained:

$$P_b \le \sum_{N=L_s}^{\infty} \sum_{X_N} \sum_{\hat{X}_N} a(X_N, \hat{X}_N) p(X_N) C_{L_\eta K} \prod_{n \in \eta} \times \left[\frac{\left(\frac{E_s}{N_0}\right)^2 [1 - J_0^2(2\pi f_d T)] + 2\left(\frac{E_s}{N_0}\right) + 1}{\left(\frac{E_s}{N_0}\right)^2 J_0^2(2\pi f_d T) d_n^2} \right]^K . \tag{45}$$

The third upper bound from (45) and (28) is

$$P_b \le \sum_{N=L_s}^{\infty} \sum_{X_N} \sum_{\hat{X}_N} \frac{a(X_N, \hat{X}_N) p(X_N)}{\alpha} \prod_{n \in \eta}$$

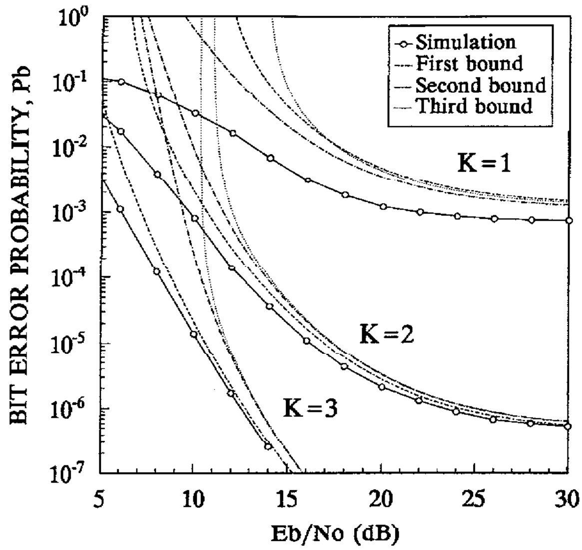

Figure 6. Bit error probability of a K-branch postdetection MRC Du/Vucetic/Zhang four state TCM–8PSK system in a Rayleigh fading channel with differential detection and a normalized fading rate of 0.03.

$$\times \left[\frac{4\left[\left(\frac{E_s}{N_0}\right)^2 [1 - J_0^2(2\pi f_d T)] + 2\left(\frac{E_s}{N_0}\right) + 1\right]}{\left(\frac{E_s}{N_0}\right)^2 J_0^2(2\pi f_d T) d_n^2} \right]^K . \tag{46}$$

Figures 5 and 6 also show the analytical results obtained through the application of these upper bounds. Figure 7 shows the simulation and analytical results for an ideal postdetection diversity differential detection system, where two consecutive symbols are assumed to fade coherently, i.e. $J_0(2\pi f_d T) = 1$.

4. Conclusion

The error performance of reference-based Maximal Ratio Combining (MRC) systems when used in conjunction with trellis-coded MPSK modulation techniques over a Rayleigh fading channel, as well as that of MRC trellis-coded MPSK systems with conventional differential detection have been analyzed. Exact and approximate expressions for the pairwise error-event probability and three upper bounds to the bit error probability in Rayleigh fading channel have been derived. Monte-Carlo simulation results, which are more indicative of the exact system performance, show that the upper bounds are very tight at high signal to noise ratios in most cases. It is found that with differential detection, Du/Vucetic/Zhang four state 8PSK system without diversity performs quite well for normalized fading rates of up to 0.03. Beyond this value, the irreducible error floor produced by differential phase jitter introduced by fading exceeds 10^{-3}. Nevertheless, the irreducible error floor is considerably lower when MRC antenna diversity is used. The problem of irreducible error floor associated with differential detection is fully eliminated at the expense of using a pilot tone aided predetection diversity coherent system. In fact, with an appropriate choice of the bandwidth of the pilot filter extractor, the performance of the pilot tone aided coded scheme is quite close to that of the idealized coherent system for normalized fading rates less than 0.03.

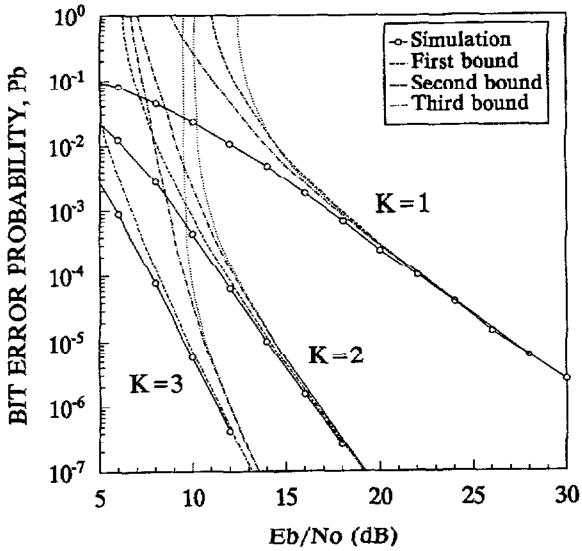

Figure 7. Bit error probability of a K-branch postdetection MRC Du/Vucetic/Zhang four state TCM–8PSK system in a Rayleigh fading channel with ideal differential detection.

Appendix

The Chernoff bound on the pairwise error probability can be obtained from (23) as [16, Appendix 4A and 4B]

$$P(X_N \to \hat{X}_N) = \Pr(f \geq 0 \mid X_N) \leq \tfrac{1}{2}\, E\{\exp(\lambda f) \mid X_N\} = \tfrac{1}{2}\, G_f(-\lambda) \qquad \text{(A.1)}$$

for any $\lambda \geq 0$, where λ is the Chernoff parameter to be optimized to get the tightest bound. For both pilot tone aided and differential systems, optimizing with respect to λ leads to

$$P(X_N \to \hat{X}) \leq \tfrac{1}{2}\, G_f(\omega_n) = \frac{1}{2} \prod_{n \in \eta} \left[1 - \frac{\omega_n^2}{t_{1n} t_{2n}}\right]^{-K}. \qquad \text{(A.2)}$$

References

1. D.G. Brennan, "Linear diversity combining techniques," Proc. IRE, Vol. 47, pp. 1075–1102, 1959.
2. W.C. Jakes, Jr., Microwave Mobile Communications. Wiley: New York. 1974.
3. S. Sampei and T. Sunaga, "Rayleigh fading compensation method for 16-QAM in digital land mobile radio channels," in Proc. IEEE 39th Veh. Technol. Conf., May 1989.
4. A. Bateman, "Feedforward transparent tone-in-band: Its implementations and applications," IEEE Trans. Veh. Technol., Vol. 39, pp. 235–243, 1990.
5. G. Ungerboeck, "Channel coding with multilevel/phase signals," IEEE Trans. Inf. Theory, Vol. IT-28, pp. 56–66, 1982.
6. D. Divsalar and M.K. Simon, "Trellis coded modulation for 4800–9600 bits/s transmission over a fading mobile satellite channel," IEEE Jour. Sel. Areas Commun., Vol. SAC-5, pp. 162–175, 1987.
7. M.K. Simon and D. Divsalar, "The performance of trellis coded multilevel DPSK on a fading mobile satellite channel," IEEE Trans. Vehic. Tech., Vol. 37, pp. 78–91, 1988.
8. D. Divsalar and M.K. Simon, "Performance of trellis-coded MDPSK on fast fading channels," in ICC'89 Conference Rec., Boston, MA, pp. 9.1.1–9.1.7, June 11–14, 1989.
9. J. Cavers and P. Ho, "Analysis of the error performance of trellis-coded modulations in Rayleigh fading channels," IEEE Trans. Commun., Vol. 40, pp. 74–83, 1992.

10. R.G. McKay, P.J. McLane and E. Biglieri, "Error bounds for trellis-coded MPSK on a fading mobile satellite channel," IEEE Trans. Commun., Vol. 39, pp. 1750–1761, 1991.
11. E. Biglieri, "High-level modulation and coding for nonlinear satellite channels," IEEE Trans. Commun., Vol. COM-32, pp. 616–626, 1984.
12. G. Femenias and R. Agustí, "Analysis of predetection diversity TCM-MPSK and postdetection diversity TCM-MDPSK systems on a Rayleigh fading channel," IEEE Trans. Commun., Vol. 43, pp. 374–385, 1995.
13. J. Du, B. Vucetic and L. Zhang, "Construction of new MPSK trellis codes for fading channels," IEEE Trans. Commun., Vol. 43, pp. 776–784, 1995.
14. K. Chan and A. Bateman, "The performance of reference-based M-ary PSK with trellis coded modulation in Rayleigh fading," IEEE Trans. Veh. Technol., Vol. 41, pp. 190–198, 1992.
15. A.J. Viterbi and J.K. Omura, Principles of Digital Communication and Coding. McGraw-Hill: 1979.
16. M.K. Simon, J.K. Omura, R.A. Scholtz and B.K. Levitt, Spread Spectrum Communications, Vol. 1, Computer Science Press: Rockville, MD. 1985.
17. J.G. Proakis, Digital Communications (2nd ed.), McGraw Hill Book Co.: Singapore. 1989.
18. J.D. Parsons and J.G. Gardiner, Mobile Communication Systems, Halsted Press; U.S.A. 1989.

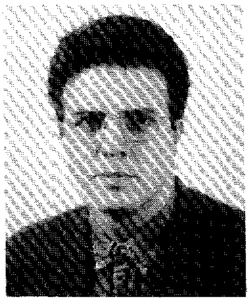

Guillem Femenias was born in Petra, Spain, on August 20, 1963. He received the Engineer and Doctor Engineer degrees in telecommunication engineering from the Universitat Politècnica de Catalunya (UPC), Spain, in 1987 and 1991, respectively.

In 1987 he joined the Departament de Teoria del Senyal i Comunicacions, Universitat Politècnica de Catalunya, Spain, where he became Associate Professor in 1990. Now he is with the Departament de Ciències Matemàtiques i Informàtica, Universitat de les Illes Balears (UIB), Spain. He has been working in the field of digital radio communications, both fixed radio relay and mobile communications. His main research interests lie in the area of communications theory with particular emphasis on trellis coded modulation, spread spectrum systems and personal, indoor and mobile radio communication systems. He has been actively participating in the COST 231 and RACE European research programs.

Ramon Agusti was born in Riba-roja d'Ebre, Spain, on 15 August 1951. He received the Engineer of Telecommunications degree from the Escuela Técnica Superior de Ingenieros de Telecommunicación de Madrid in1973 and the Doctor Engineering degree from the Universitat Politècnica de Catalunya (Barcelona) in 1978. In 1973 he joined the Escuela Técnica Superior de Ingenieros de Telecomunicación de Barcelona where he became Full Professor in 1987.

He has been working in the field of digital communications with particular emphasis on transmission and development aspects in digital radio, both fixed radio delay and mobile communications. At present his research interest lies in the area of personal communication systems. He has published about 40 papers and participated in about 20, both private and governmental, funded projects on these fields. In particular he is now participating in the European COST 231 and ACTS programs.